

Cluster radioactivity in ²¹⁰⁻²²⁶Ra isotopes

K. P. Santhosh,* Sabina Sahadevan, B. Priyanka, M. S. Unnikrishnan,
Jayesh George Joseph and R. K. Biju

School of Pure and Applied Physics, Kannur University, Payyanur Campus, Payyanur – 670327, INDIA

* email: drkpsanthosh@gmail.com

Introduction

The study of radium isotopes in the field of cluster decay is prominent because due to their position in the trans-lead region in the nuclear chart, the role of the doubly magic ²⁰⁸Pb and its immediate neighbors as one of the decay fragments comes into play when cluster emission occurs. In fact experimentally ¹⁴C spontaneous emission from radium isotopes is one of the most observed cluster decay modes. In this paper the cluster emission of ²¹⁰⁻²²⁶Ra isotopes has been studied within the Coulomb and proximity potential model [1] with a view to analyze the spherical shell closures in the daughter lead region.

The Coulomb and proximity potential model

The interacting potential barrier for a parent nuclei exhibiting cluster radioactivity is given by $V = Z_1 Z_2 e^2 / r + V_p(z)$ for $Z > 0$ (1)

Here Z_1 and Z_2 are the atomic numbers of daughter and emitted cluster, r is the distance between the fragment centers and z is the distance between the near surfaces of the fragments and V_p is the proximity potential given by Blocki et al [2].

The barrier penetrability P is given as

$$P = \exp \left\{ - \frac{2}{\hbar} \int_a^b \sqrt{2\mu(V-Q)} dz \right\} \quad (2)$$

The inner and outer turning points a and b are defined as $V(a) = V(b) = Q$, where Q is the energy released and μ the reduced mass. The half life time is given by,

$$T_{1/2} = \ln 2 / \lambda = \ln 2 / nP \quad (3)$$

Here λ is the decay constant and assault frequency, $n = 2E_V / h$. The empirical zero point vibration energy is given as [3]

$$E_V = Q \{ 0.056 + 0.039 \exp[(4 - A_2) / 2.5] \} \quad (4)$$

for $A_2 \geq 4$

Results and discussion

The decay studies starts with the identification of the probable clusters from the ²¹⁰⁻²²⁶Ra isotopes through the cold valley plots. From the cold valley plots it is observed that the clusters most probable for emission from all the radium isotopes are the typical clusters of ⁴He, ^{8,10}Be, ^{12,14}C, ^{18,20}O, ^{22,24}Ne, ^{26,28}Mg etc. In addition to the dips at these usual clusters, the Ca valley with ⁴⁶⁻⁵²Ca nuclei as the probable clusters also appear in the cold valley plots of all the parent isotopes. These valleys signify the role of the $Z = 20$, $N = 28$ magicities in the Ca nuclei. Another valley which appears in all the graphs is the one at the Sr clusters which are of course due to the $Z = 50$ spherical shell closure in the corresponding Sn daughter fragments. Also a third valley comes up at the Ni cluster for ²¹⁰Ra but it gets shifted to Zn cluster for ²¹²Ra until it merges with the Sr valley as a dip at ⁹²Kr in the cold valley graph for ²²⁶Ra. This happens so because this deep valley is due to the $N = 82$ magic number in the daughter nuclei.

After identification of the most probable clusters from the driving potential versus A_2 graphs the decay characteristics are computed within CPPM. The penetrability, decay constant and half lives for the emission of various clusters from the ²¹⁰⁻²²⁶Ra parent isotopes are calculated and $\log_{10}(T_{1/2})$ is displayed in Figure 1. The experimental $\log_{10}(T_{1/2})$ values are compared with the CPPM values wherever data is available and they are in good agreement as can be seen from Figure 1.

For e.g. for the case of α -decay from ^{214}Ra $\{\log_{10}(T_{1/2})\}_{\text{calc.}}=0.48$ and $\{\log_{10}(T_{1/2})\}_{\text{expt.}}=0.39$, for α -decay from ^{216}Ra $\{\log_{10}(T_{1/2})\}_{\text{calc.}}=-6.58$ and $\{\log_{10}(T_{1/2})\}_{\text{expt.}}=-6.74$ and for α -decay from ^{222}Ra $\{\log_{10}(T_{1/2})\}_{\text{calc.}}=2.76$ and $\{\log_{10}(T_{1/2})\}_{\text{expt.}}=1.58$ respectively.

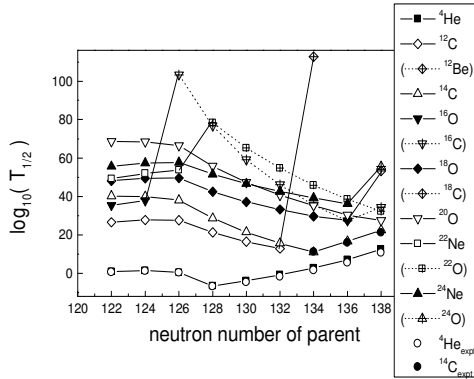


Fig. 1 Plot of the computed $\log_{10}(T_{1/2})$ values vs. neutron number of parent for ^4He , ^{12}C , ^{14}C , ^{16}O , ^{18}O and $^{22,24}\text{Ne}$ clusters from Ra isotopes.

For the case of ^{14}C decay from ^{222}Ra $\{\log_{10}(T_{1/2})\}_{\text{calc.}}=11.02$ and $\{\log_{10}(T_{1/2})\}_{\text{expt.}}=11.1$, for ^{14}C decay from ^{224}Ra $\{\log_{10}(T_{1/2})\}_{\text{calc.}}=16.67$ and $\{\log_{10}(T_{1/2})\}_{\text{expt.}}=15.89$ and for ^{14}C decay from ^{226}Ra $\{\log_{10}(T_{1/2})\}_{\text{calc.}}=22.53$ and $\{\log_{10}(T_{1/2})\}_{\text{expt.}}=21.2$. The experimental $T_{1/2}$ values are obtained from Ref. [4]. In Figure 1, a slight rise in $T_{1/2}$ values is got for all the clusters at $N = 126$ signifying the well established spherical shell closure there. The graph is also showing dips at certain neutron numbers thereby denoting the shell closure in the daughter nucleus there. The first dip is got at ^{216}Ra parent ($N = 128$) for the alpha decay and this is due to the $N = 126$ magicity in the ^{212}Rn daughter. Then there are dips at $N = 132, 134$ and 136 ($^{222, 224, 226}\text{Ra}$) for ^{12}C , ^{14}C and ^{16}C emissions respectively. All the three decrease in half lives are due to the double magicity ($Z = 82, N = 126$) of the well known ^{208}Pb daughters. Two other dips are observed at the ^{224}Ra ($N = 136$) parent for the decay of ^{18}O and ^{24}Ne emissions respectively. The first one is due to the $N = 126$ spherical closure in the ^{206}Hg daughter and the second one is due to $Z \approx 76$ major (deformed) closed shell in the ^{200}Pt daughter nucleus.

Figure 2 displays similar plot for $^{26,28}\text{Mg}$, $^{30,32,34}\text{Si}$ and $^{36,38,40}\text{S}$ cluster emissions. Here too

there is a rise in $T_{1/2}$ values at $N = 126$ which is expected. Dips are seen at $N = 128$ (^{216}Ra) for ^{36}S decay at $N = 130$ for ^{32}Si and ^{38}S decays respectively. The dip for ^{36}S emission is due to the $Z = 72$ major (deformed) shell closure in ^{180}Hf daughter while the dips at $N = 130$ (^{220}Ra) for ^{32}Si and ^{38}S decays are due to the $Z = 74, 72$ major (deformed) shell closures in ^{186}W and ^{180}Hf daughters respectively. Again a dip can be seen at ^{222}Ra parent ($N = 134$) for ^{40}S decay and

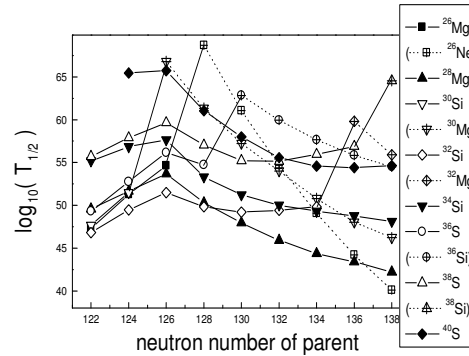


Fig. 2 Plot of the computed $\log_{10}(T_{1/2})$ values vs. neutron number of parent for $^{26,28}\text{Mg}$, $^{30,32,34}\text{Si}$ and $^{36,38,40}\text{S}$ clusters from Ra isotopes.

this is also due to the $Z = 72$ deformed shell closure in the ^{182}Hf daughter fragment. The $Z = 76, 74, 72$ are major (deformed) shell closures which are predicted by Santhosh et.al [5] and references therein. Therefore the study on Ra isotopes is exhibiting all the known spherical shell closures in the relevant part of the nuclear chart and together with it some major (deformed) shell closures are also coming up from the half lives graphs.

References

- [1] K. P. Santhosh and Antony Joseph, Pramana-J. Phys **58**, 611 (2002).
- [2] J. Blocki et al, Ann. Phys (N.Y) **105**, 427 (1977).
- [3] D. N. Poenaru, M. Ivascu, A. Sandulescu and W. Greiner, Phys. Rev. **C 32**, 572 (1985).
- [4] NuDat2.5, <http://www.nndc.bnl.gov>
- [5] K. P. Santhosh and Sabina Sahadevan Nucl. Phys. A **847** 42 (2010).